Journal of Zhejiang University SCIENCE A
ISSN 1673-565X (Print); ISSN 1862-1775 (Online)
www.zju.edu.cn/jzus; www.springerlink.com
E-mail: jzus@zju.edu.cn

Estimation of vegetation biophysical parameters by remote sensing using radial basis function neural network*

YANG Xiao-hua[†1,4], HUANG Jing-feng[†‡1,4], WANG Jian-wen[2], WANG Xiu-zhen[3], LIU Zhan-yu[1,2]

([1]*Institute of Agricultural Remote Sensing & Information Application, Zhejiang University, Hangzhou 310029, China*)

([2]*Communication Training Base of General Staff Headquarters, Beijing 102400, China*)

([3]*Zhejiang Meteorological Institute, Hangzhou 310004, China*)

([4]*Key Laboratory of Agricultural Remote Sensing & Information System, Hangzhou 310029, China*)

[†]E-mail: yxhua1@tom.com; hjf@zju.edu.cn

Received Sept. 8, 2006; revision accepted Nov. 24, 2006

Abstract: Hyperspectral reflectance (350~2500 nm) data were recorded at two different sites of rice in two experiment fields including two cultivars, and three levels of nitrogen (N) application. Twenty-five Vegetation Indices (VIs) were used to predict the rice agronomic parameters including Leaf Area Index (LAI, m^2 green leaf/m^2 soil) and Green Leaf Chlorophyll Density (GLCD, mg chlorophyll/m^2 soil) by the traditional regression models and Radial Basis Function Neural Network (RBF). RBF emerged as a variant of Artificial Neural Networks (ANNs) in the late 1980's. A large variety of training algorithms has been tested for training RBF networks. In this study, Original RBF (ORBF), Gradient Descent RBF (GDRBF), and Generalized Regression Neural Network (GRNN) were employed. Results showed that green waveband Normalized Difference Vegetation Index ($NDVI_{green}$) and TCARI/OSAVI have the best prediction power for LAI by exponent model and ORBF respectively, and that TCARI/OSAVI has the best prediction power for GLCD by exponent model and GDRBF. The best performances of RBF are compared with the traditional models, showing that the relationship between VIs and agronomic variables are further improved when RBF is used. Compared with the best traditional models, ORBF using TCARI/OSAVI improves the prediction power for LAI by lowering the Root Mean Square Error (RMSE) for 0.1119, and GDRBF using TCARI/OSAVI improves the prediction power for GLCD by lowering the RMSE for 26.7853. It is concluded that RBF provides a useful exploratory and predictive tool when applied to the sensitive VIs.

Key words: Artificial neural network (ANN), Radial basis function (RBF), Remote sensing, Rice, Vegetation index (VI)
doi:10.1631/jzus.2007.A0883 **Document code:** A **CLC number:** TP751

INTRODUCTION

Measurement of various canopy crop variables during the growing season provides an opportunity for improving grain yields and quality by site-specific application of fertilizers (Jamieson *et al*., 1998; Asseng *et al*., 2000). The spatial and temporal variations in the field of these variables must be determined in order to match the crop requirements as closely as possible.

Different remote sensing applications have proved to be a potential source of reflectance data for estimation of several canopy variables related to biophysical, physiological or biochemical characteristics (Ahlrichs and Bauer, 1983; Serrano *et al*., 2000; Thenkabail *et al*., 2000; Cheng *et al*., 2003; Tang, *et al*., 2004; Zhang, *et al*., 2006). Various Vegetation Indices (VIs) have been related to crop variables such as biomass, leaf area, plant cover, leaf gap fraction, nitrogen, and chlorophyll in cereals (Best and Harlan, 1985; Christensen and Goudriaan, 1993; Lukina *et al*., 1999; Aparicio *et al*., 2000; Cheng, 2006). The Ratio Vegetation Index (RVI; Pearson and Miller, 1972) and the Normalized Difference Vegetation Index

‡ Corresponding author
* Project (Nos. 40571115 and 40271078) supported by the National Natural Science Foundation of China

(NDVI; Rouse *et al*., 1974) are the best-known indices. To reduce the background effect, many VIs have been proposed. These VIs include the Soil-Adjusted Vegetation Index (SAVI; Huete, 1988), the Modified SAVI (MSAVI; Qi *et al*., 1994), the Transformed Chlorophyll Absorption in Reflectance Index (TCARI; Kim *et al*., 1994), the Modified Chlorophyll Absorption in Reflectance Index (MCARI; Daughtry *et al*., 2000), and the Optimized SAVI (OSAVI) (Rondeaux *et al*., 1996). In order to enhance information related to Leaf Area Index (LAI) and Green Leaf Chlorophyll Density (GLCD), the TCARI/OSAVI ratio was defined by Haboudane *et al*.(2002). $NDVI_{green}$ was introduced in (Gitelson *et al*., 1996), and the Modified Chlorophyll Absorption Continuum Index (MCACI) was presented by Yang *et al*.(2006), and so on. Many studies have focused on estimation of crop LAI and GLCD (Broge and Leblanc, 2001; Curran *et al*., 2001; Boegh *et al*., 2002; Broge and Mortensen, 2002; Haboudane *et al*., 2002; Gong *et al*., 2003) using VIs. But these VIs were seldom used to study the relationships between rice agronomic parameters and rice canopy reflectance.

Artificial Neural Networks (ANNs) are relatively crude electronic models based on the neural structure of the brain. The brain basically learns from experience. It is natural proof that some problems beyond the scope of current computers are indeed solvable by small energy efficient packages. This brain modeling also promises a less technical way to develop machine solutions.

Radial Basis Functions (RBFs) emerged as a variant of ANN in the late 1980's. However, their roots are entrenched in much older pattern recognition techniques such as potential functions, clustering, functional approximation, spline interpolation and mixture models (Tou and Gonzalez, 1974). Later, a large variety of training algorithms has been tested for training RBF networks. In the initial approaches, an RBF was assigned for each data sample, which proved to be expensive in terms of memory requirement and the number of parameters. On the other hand, exact fit to the training data may cause bad generalization. Other approaches choose randomly or assumed known hidden unit weights and calculate the output weights by solving a system of equations whose solution is given in the training set (Broomhead and Lowe, 1988). The matrix inversion required in this approach is computationally expensive and could cause numerical problems in certain situations (when the matrix is singular). The RBF centers are uniformly distributed in the data space (Matej and Lewitt, 1996). The function to be modeled is obtained by interpolation. Less basis functions are used for given data samples (Niranjan and Fallside, 1990). A least squares solution that minimizes the interpolation error is proposed. Orthogonal least squares using Gram-Schmidt algorithm was proposed in (Chen *et al*., 1991). An adaptive training algorithm for minimizing a given cost function is a gradient descent algorithm. Expectation-maximization algorithm using a gradient descent algorithm for modeling the input-output distributions was employed in (Cha and Kassam, 1996). Clustering algorithms such as *k*-means (Tou and Gonzalez, 1974) and learning vector quantization (Kohonen, 1989) were employed for finding the hidden unit parameters in (Moody, 1989). Other approaches employ cluster merging (Musavi *et al*., 1992) or splitting (Bors and Gabbouj, 1994).

RBF networks have been successfully applied to a large diversity of applications including interpolation (Broomhead and Lowe, 1988; Matej and Lewitt, 1996), chaotic time-series modeling (Casdagli, 1989; Moody, 1989), system identification, control engineering (Sanner and Slotine, 1992), electronic device parameter modeling, channel equalization (Chen *et al*., 1991; Bors and Gabbouj, 1994; Haykin, 1994), speech recognition (Niranjan and Fallside, 1990; Bors and Gabbouj, 1994), image restoration (Cha and Kassam, 1996), shape-from-shading (Wei and Hirzinger, 1997), 3D object modeling (Matej and Lewitt, 1996; Bors and Pitas, 1999), motion estimation and moving object segmentation (Bors and Pitas, 1998), data fusion (Chatzis *et al*., 1999), etc. A little of our knowledge has been applied to RBF to estimate the rice agronomic parameters using remote sensing data.

The objectives of the present investigation were to compare the prediction power between the best traditional model and RBF technique of each VI for agronomic parameters. The VIs are independent variables in traditional models and are used as net inputs in RBF, and the agronomic parameters are dependent variables in traditional models and are used as net outputs in RBF. All models were fitted to two different agronomic variables: LAI and GLCD in rice.

MATERIALS AND METHODS

Study area

The study area is located at Zhejiang University Experiment Field, Hangzhou, Zhejiang Province, China, located at 120°10'05" E, 30°14'03" N. In order to acquire a big variation in LAI and GLCD in rice, two field experiments with different rates of nitrogen fertilization and different rice cultivars were carried out in 2004. The first experiment was earlier than the second experiment by half a month. Winter oilseed rape and rice were included in the crop rotations on the two experimental fields. The straw was usually removed from the field. The study area is characterized by monsoon climate with hot summer and cool winter. The average annual rainfall is 1374.7 mm and the average annual temperature is 17.8 °C. The soil is sandy loam paddy soil with pH 5.7, organic matter content of 16.5 g/kg and total N of 1.02 g/kg.

Field experimental design

In an experiment, two cultivars of rice, 'Xiushui 110' and 'Xieyou 9308' were used. Each cultivar was seeded to a plant density of 45 plants/m^2. Furthermore, this plant density level was furthermore split into twelve with every four of these subplots receiving 0, 120, 240 kg N/ha, respectively, so each N level had four replicates. The plots number of the two experiments was 48 and the plot size was 4.60 m×5.46 m. The first experiment was carried out around May 30th, 2004 and the second experiment around June 15th, 2004, in well-cultivated soil with seeding depth of 3 cm, and transplanted one month later respectively. Nitrogen fertilizer (urea) was applied as 45% base fertilizer, 35% tillering fertilizer, and 20% heading fertilizer; and the treatment levels represented no-nitrogen fertilizer, a proper application and a superabundant dose. In addition, 225 kg $Ca(H_2PO_4)_2$/ha was applied as a base fertilizer with 150 kg KCl/ha as a tillering fertilizer and 150 kg KCl/ha as a heading fertilizer.

Spectral measurements

Canopy reflectance was ground-based and measured using a spectroradiometer in a range from 350 nm to 2500 nm, manufactured by Analytical Spectral Devices^{TM} and 2 m above ground. The spectroradiometer had spectral resolutions of 3 nm between 400 nm and 1000 nm, and about 10 nm between 1000 and 2500 nm. Due to severe noise in the water absorption spectrum from 1330 nm to 1480 nm and from 1780 nm to 1990 nm, only the data collected in 350~1330 nm, 1480~1780 nm, and 1990~2300 nm were used. The band centers were rounded off to the nearest whole number (e.g., 549.50 nm as 550 nm). The spectroradiometer unit consisted of a main spectrometer, a personal computer, fiber optic cable, a pistol grip, and different field of view (FOV) cones. Inside the spectrometer, light is projected from the fiber optics onto a holographic diffraction grating where wavelength components are separated and reflected for independent collection by the detector(s). The observation of rice spectra and agronomic variables were performed between 1100 and 1400 local time (GMT+8) on 20 July, 8 Aug., 28 Aug., 22 Sept., 5 Oct. and 27 Oct. of 2004 for the first experiment, and on 8 Aug., 28 Aug., 22 Sept., 5 Oct. and 27 Oct. of 2004 for the second experiment. All rice fields were filled with water except on 27 Oct. for the two experiments. At each plot, 10 reflectance measurements were consistently taken, with a nadir view from a height of 1.0 m above the canopy, using a 25° FOV. The measurement sites were selected randomly at each plot. This resulted in viewing an area of 1544 cm^2 at the canopy level. Spectroradiometer data of rice were analyzed using softwares PORT-SPECTM and VNIRTM supplied by the manufacturer of the instrument (Analytical Spectral Devices^{TM}), and Statistical Analysis System (SPSS) version 11.5. The target reflectance is the ratio of energy reflected off the rice to energy incident on the $BaSO_4$ white reference [Eq.(1)]. Since the dark current varies with time and temperature, it was collected for each integration time (virtually for each new reading). The solar angle compared to nadir was for all measurements less than 45º and no disturbing clouds were observed.

$$\text{Reflectance (\%)}=\frac{\text{target}-\text{dark current}}{\text{reference}-\text{dark current}}\times 100\%. \quad (1)$$

Plant sampling and harvest procedure

Green plant sampling was performed many times during the vegetative growth stages from early stem elongation until heading. The actual dates were the same as the dates of canopy reflectance performed.

At the rice field, a representative area of 0.088 m^2 was cut above ground and brought to the lab for weight determination and calculation of the rice agronomic parameters. All representative samples were taken and the weights were determined. Then, Leaves Length (*LL*, cm) and Leaves Width (*LW*, cm) were measured. Green Leaf Fresh Weights (*GLFW*) per square soil meter were determined (g/m^2). Based on these measurements, *LAI* (cm^2/cm^2) was calculated:

$$LAI=\sum(LL\times LW\times 0.83)/(0.088\times 10\,000), \quad (2)$$

where 0.83 is the rice leaf calibration coefficient.

Leaves and stems were separated by excision at the leaf base. One leaf was randomly selected among the youngest fully developed leaves to carry out the organic extraction of leaf chlorophyll. The leaves samples were chipped, weighted and then dipped in 20 ml mixed solution (acetone:ethanol:distilled water=4.5:4.5:1) for 24 h to extract chlorophyll of rice leaves. The Optical Density (*OD*) of the extract was measured at 663 nm and 645 nm by Spectrophotometer (BACKMAN DU 600). The concentrations (mg/L) of *Chla*, *Chlb* and total chlorophyll (*Chlt*=*Chla*+*Chlb*) in the extract were calculated by using the following Eqs.(3)~(5) and the contents (mg/g) of chlorophyll were calculated by Eq.(6):

$$Chla\ (\text{mg/L})=12.7OD_{663}-2.69OD_{645}, \quad (3)$$

$$Chlb\ (\text{mg/L})=22.9OD_{645}-4.68OD_{663}, \quad (4)$$

$$Chlt\ (\text{mg/L})=8.02OD_{663}+20.21OD_{645}, \quad (5)$$

$$GLCC\ (\text{mg/g})=C_c\ (\text{mg/L})\times[V\ (\text{ml})/1000]/M\ (\text{g}), \quad (6)$$

where *GLCC*, C_c, *V* and *M* are green leaf chlorophyll content (mg/g), pigment concentration (mg/L), volume (ml) of the abstraction in the solution and mass (g) of the sample, respectively.

The *GLCD* (mg chlorophyll/m^2 soil) was calculated by

$$GLCD\ (\text{mg/m}^2)=GLCC\times GLFW/0.088. \quad (7)$$

Vegetation indices

The basic models that correlate with agronomic variables are VIs. In this study, 25 VIs were used in four traditional models against those of LAI and GLCD. Their expressions are listed in Table 1. The width of NIR, Red, Green bands that are used in all VIs corresponded to the bands of a Ladsat-5^{TM} sensor, and their values are average values of all bands.

Radial basis functions

Radial Basis Functions Neural Network (RBFs) was proposed by Broomhead and Lowe (1988). This neural network is very different from neural networks with sigmoidal activation functions in that it utilizes basis functions in the hidden layer that are locally responsive to input stimulus. RBFs are embedded in a two-layer neural network, where each hidden unit implements a radial activated function. The output units implement a weighted sum of hidden unit outputs. The input into an RBF network is nonlinear while the output is linear. Their excellent approximation capabilities have been studied in (Poggio and Girosi, 1990; Park and Sandberg, 1991). Due to their nonlinear approximation properties, RBF networks can model complex mappings, which perceptron neural networks can only model by means of multiple intermediary layers (Haykin, 1994).

In order to use an RBF network, we need to specify the hidden unit activation function, the number of processing units, a criterion for modeling a given task and a training algorithm for finding the parameters of the network. Finding the RBF weights is called network training. If we have at hand a set of input-output pairs, called training set, we optimize the network parameters in order to fit the network outputs to the given inputs. The fit is evaluated by means of a cost function, usually assumed to be the mean square error. After training, the RBF network can be used with data whose underlying statistics is similar to that of the training set. Online training algorithms adapt the network parameters to the changing data statistics (Moody, 1989; Bors and Pitas, 1996). A large variety of training algorithms has been tested for training RBF networks. In this study, Original RBF (ORBF), Gradient Descent RBF (GDRBF), and Generalized Regression Neural Network (GRNN) were employed.

Measurement of model performance

Usually the analysis of model performance was conducted by comparing the correlation coefficient (*R*), average absolute error (*ABSE*) and root mean squared error (*RMSE*) between the predicted sets and the corresponding observed sets in most literature

Table 1 The expressions of all VIs in this study

Acronym	Vegetation Index	Reference	Eq. ID
RVI	$RVI=NIR/Red$	Pearson and Miller, 1972	(8)
NDVI	$NDVI=(NIR-Red)/(NIR+Red)$	Rouse *et al*., 1974	(9)
$NDVI_{green}$	$NDVI_{green}=(NIR-Green)/(NIR+Green)$	Gitelson *et al*., 1996	(10)
SAVI	$SAVI=1.5(NIR-Red)/(NIR+Red+0.5)$	Huete, 1988	(11)
OSAVI	$OSAVI=(NIR-Red)/(NIR+Red+0.16)$	Rondeaux *et al*., 1996	(12)
MSAVI	$MSAVI=\{2NIR+1-[(2NIR+1)^2-8(NIR-Red)]^{1/2}\}/2$	Qi *et al*., 1994	(13)
MCACI	$MCACI=\sum_{\lambda_i}^{\lambda_n}(R_i^c-R_i)\Delta\lambda_i$	Yang *et al*., 2006	(14)
TCARI	$TCARI=3[(R_{700}-R_{670})-0.2(R_{700}-R_{550})R_{700}/R_{670}]$	Kim *et al*., 1994	(15)
TCARI/OSAVI	*TCARI/OSAVI*	Haboudane *et al*., 2002	(16)
RDVI	$RDVI=(NIR-Red)/\sqrt{NIR+Red}$	Roujean and Breon, 1995	(17)
RVI_2	$RVI_2=NIR/Green$	Gitelson *et al*., 1996	(18)
$RVI_{750/700}$	$RVI_{750/700}=R_{750}/R_{700}$	Gitelson *et al*., 1996	(19)
$RVI_{750/550}$	$RVI_{750/550}=R_{750}/R_{550}$	Gitelson *et al*., 1996	(20)
$RVI_{800/600}$	$RVI_{800/600}=R_{800}/R_{600}$	Sims and Gamon, 2002	(21)
DVI	$DVI=NIR-Red$	Jordan, 1969	(22)
TVI	$TVI=\sqrt{NDVI+0.5}$	Rouse *et al*., 1974	(23)
SIPI	$SIPI=(R_{800}-R_{445})/(R_{800}+R_{680})$	Peňuelas *et al*., 1995	(24)
VI_{700}	$VI_{700}=(R_{700}-Red)/(R_{700}+Red)$	Gitelson *et al*., 2002	(25)
NLI	$NLI=(NIR^2-Red)/(NIR^2+Red)$	Goel and Qi, 1994	(26)
$RDVI_1$	$RDVI_1=\sqrt{NDVI\times(NIR-Red)}$	Roujean and Breon, 1995	(27)
MSR	$MSR=(NIR/Red-1)/(\sqrt{NIR/Red}+1)$	Gong *et al*., 2003	(28)
MNLI	$MNLI=(NIR^2-Red)(1+0.5)/(NIR^2+Red+0.5)$	Gong *et al*., 2003	(29)
TVI_2	$TVI_2=60(NIR-Green)-100(Red-Green)$	Broge and Leblanc, 2000	(30)
SAVI×SR	$SAVI\times SR=(NIR^2-Red)/(NIR+Red+L)\times Red$, $L=0.5$	Gong *et al*., 2003	(31)
$VARI_{700}$	$VARI_{700}=(R_{700}-1.7Red+0.7Blue)/(R_{700}+2.3Red-1.3Blue)$	Gitelson *et al*., 2002	(32)

(O'Neal *et al*., 2002; Mutanga and Skidmore, 2004). The calculated R statistic is defined as the proportion of variance of the response that can be explained by the regressor variable(s). However, the R statistic can be misleading when comparing experiment results on the same variable but with different ranges for the regressors (Broge and Mortensen, 2002), such as the experiment reported herein. In such cases, one should look at *ABSE* and *RMSE* rather than at R. For these reasons, we decided to compare the results on the *RMSE* and *ABSE*. They are defined as follows:

$$RMSE=\sqrt{\sum(P-P')^2/(N-1)}, \quad (33)$$

$$ABSE=\sum[\mathrm{abs}(P-P')]/N, \quad (34)$$

where P' is the simulated value of *LAI* and *GLCD* of rice, P is the measured value of *LAI* and *GLCD* of rice, and N is the number of test samples.

RESULTS

Statistical description of the measured data

The experimental treatments, including different cultivars, plant densities, and nitrogen application strategies together with the temporal timing of plant sampling, caused a wide range of variation within the investigated crop variables, i.e., there were almost 18-fold variation in LAI and 93-fold variation in GLCD (Table 2). The wide range in the investigated crop variables was planned to make the relationship between plant performance and reflectance measurements as realistic and universal as possible.

Table 2 Selected properties of the investigated rice *LAI* and rice *GLCD*

Variable	Mean	Min	Max	Range*
LAI (m^2/m^2)	3.59	0.47	8.27	7.80
GLCD (mg/m^2)	1162.41	31.83	2970.06	2938.23

* Difference between the maximum and the minimum

Selection of the best models

The relationships between all VIs and agronomic parameters were studied using four traditional models. In this process, all samples (182) were used, all R^2 have been calculated. The results are listed in Table 3.

The highlighted R^2 values indicate the better relationships between VIs and agronomic parameters. The best model is selected based on R^2 value for each VI excluding the VIs with all R^2 values smaller than 0.6. The results are listed in Table 4. These models were used for further study.

Results of the best traditional models

There are totally 182 samples in the study. Samples of the two experiments were combined into one dataset, and then it was divided randomly into two sub-datasets. The first sub-dataset (100 samples) was used for building models, and the second sub-dataset (82 samples) for measuring the effectiveness of the models. Results of all the best models for all LAI and only three for GLCD (due to space limitation) are listed in Fig.1 and Fig.2 respectively, and their assessments including *R*, *ABSE* and *RMSE* are listed in Table 5.

Table 4 The best model for each VI with R^2>0.6

	Vegetation Index	Model	R^2
LAI	RVI_2	Power	0.6214
	$NDVI_{green}$	Exponent	0.6219
	TCARI/OSAVI	Power	0.6311
GLCD	*RVI*	Power	0.6419
	NDVI	Exponent	0.7206
	$NDVI_{green}$	Exponent	0.8085
	SAVI	Exponent	0.7206
	OSAVI	Power	0.7253
	MSAVI	Power	0.6940
	MCACI	Power	0.6257
	TCARI/OSAVI	Exponent	0.7440
	RDVI	Power	0.7112
	RVI_2	Power	0.7804
	$RVI_{750/700}$	Power	0.6229
	$RVI_{800/600}$	Power	0.6056
	DVI	Power	0.6594
	TVI	Power	0.7236
	NLI	Exponent	0.7166
	$RDVI_1$	Power	0.7334
	MSR	Power	0.6773
	TVI_2	Power	0.6317

Table 3 The R^2 values of four traditional models between VIs and LAI, GLCD of rice

Vegetation Index	R^2							
	LAI				*GLCD*			
	Linearity	Exponent	Power	Logarithm	Linearity	Exponent	Power	Logarithm
RVI	0.2772	0.3262	0.4542	0.3653	0.3494	0.4422	**0.6419**	0.4457
NDVI	0.3809	0.4932	0.4749	0.3571	0.4503	**0.7206**	**0.7161**	0.4133
$NDVI_{green}$	0.4867	**0.6219**	0.5739	0.4359	0.5225	**0.8085**	**0.7851**	0.4645
SAVI	0.3809	0.4932	0.4749	0.3581	0.4503	**0.7206**	**0.7161**	0.4133
OSAVI	0.3821	0.4819	0.4697	0.3632	0.4447	**0.7060**	**0.7253**	0.4160
MSAVI	0.3410	0.4168	0.4477	0.3545	0.3936	0.5989	**0.6940**	0.4058
MCACI	0.2813	0.3219	0.3735	0.3199	0.3352	0.4814	**0.6257**	0.3905
TCARI	0.1782	0.1889	0.1621	0.1687	0.1452	0.0977	0.0807	0.1371
TCARI/OSAVI	0.4807	**0.6072**	**0.6311**	0.5351	0.4936	**0.7440**	**0.7423**	0.5515
RDVI	0.3654	0.4562	0.4583	0.3575	0.4217	**0.6674**	**0.7112**	0.4081
RVI_2	0.4757	0.5382	**0.6214**	0.5078	0.5182	**0.6396**	**0.7804**	0.5497
$RVI_{750/700}$	0.3041	0.3491	0.4326	0.3603	0.3767	0.4788	**0.6229**	0.4422
$RVI_{750/550}$	0.4012	0.4601	0.1937	0.2545	0.4241	0.5427	0.3685	0.2013
$RVI_{800/600}$	0.2426	0.2929	0.4171	0.3321	0.3210	0.4130	**0.6056**	0.4198
DVI	0.3111	0.3792	0.4172	0.3323	0.3523	0.5538	**0.6594**	0.3768
TVI	0.3772	0.4915	0.4878	0.3720	0.4431	**0.7234**	**0.7236**	0.4342
SIPI	0.0868	0.1009	0.0986	0.0859	0.1604	0.2985	0.2949	0.1634
VI_{700}	0.2140	0.3143	0.3398	0.2305	0.2915	0.4795	0.4990	0.2922
NLI	0.3886	0.4847	–	–	0.4633	**0.7166**	–	–
$RDVI_1$	0.3948	0.4928	0.4862	0.3786	0.4441	**0.6959**	**0.7334**	0.4231
MSR	0.3221	0.3910	0.4705	0.3666	0.4071	0.5430	**0.6773**	0.4418
MNLI	0.3292	0.4053	–	–	0.3775	0.5632	–	–
TVI_2	0.2809	0.3422	0.3868	0.3090	0.3274	0.5214	**0.6317**	0.3585
SAVI×SR	0.2612	0.3045	–	–	0.3213	0.4124	–	–
$VARI_{700}$	0.0888	0.1257	0.1553	0.1127	0.1724	0.2709	0.3327	0.1970

Note: the highlighted R^2 values indicate the better relationships between VIs and agronomic parameters

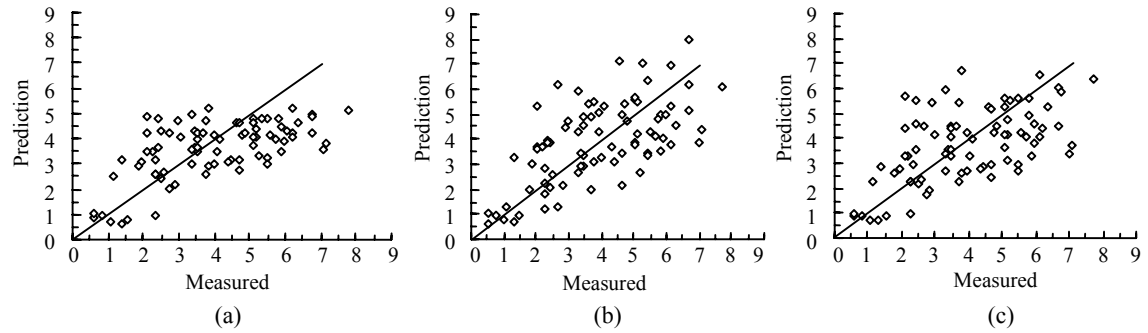

Fig.1 Scatter plots of the prediction (*y* axis) and the measured (*x* axis) *LAI* using the testing data for three VIs. (a) $NDVI_{green}$ on exponent model; (b) TCARI/OSAVI on power model; (c) RVI_2 on power model. The line is *y=x*

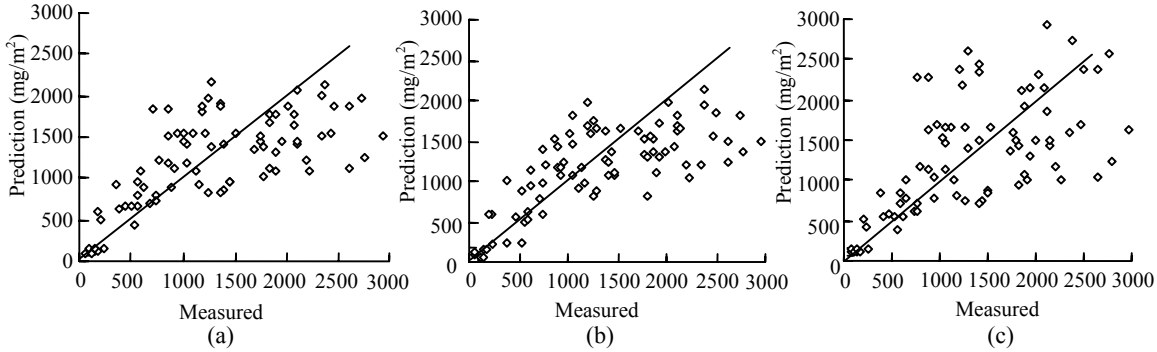

Fig.2 Scatter plots of the prediction (*y* axis) and the measured (*x* axis) *GLCD* using the testing data only for three VIs. (a) $NDVI_{green}$ on exponent model; (b) TCARI/OSAVI on exponent model; (c) RVI_2 on power model. The line is *y=x*

Table 5 The assessment results of traditional models for *LAI* and *GLCD* of rice

	Vegetation Index	Equation	R^2	*RMSE*	*R*	*ABSE*	Eq. ID
LAI	$NDVI_{green}$	$LAI=0.2993\exp(3.3724NDVI_{green})$	0.6492	1.4003	0.6176	1.1567	(35)
	TCARI/OSAVI	$LAI=0.2381(TCARI/OSAVI)^{-1.4252}$	0.6509	1.4334	0.6395	1.1905	(36)
	RVI_2	$LAI=0.4543(RVI_2)^{1.0749}$	0.6639	1.4843	0.5844	1.1773	(37)
GLCD	*RVI*	$GLCD=49.661RVI^{1.2657}$	0.6632	754.9633	0.5088	564.7806	(38)
	NDVI	$GLCD=12.969\exp(5.4209NDVI)$	0.7361	638.8190	0.5952	511.7610	(39)
	$NDVI_{green}$	$GLCD=16.065\exp(5.7666NDVI_{green})$	0.8237	566.5862	0.6843	439.2791	(40)
	SAVI	$GLCD=12.692\exp(3.6139SAVI)$	0.7361	638.9193	0.5952	511.7878	(41)
	OSAVI	$GLCD=3317.1OSAVI^{2.538}$	0.7479	679.6662	0.5608	527.5220	(42)
	MSAVI	$GLCD=3815.8MSAVI^{1.814}$	0.7284	730.3528	0.4701	564.9251	(43)
	MCACI	$GLCD=85.351MCACI^{1.0785}$	0.6289	723.6685	0.4658	569.2385	(44)
	TCARI/OSAVI	$GLCD=4943.4\exp(-9.8749TCARI/OSAVI)$	0.7406	554.2854	0.7209	427.8513	(45)
	RDVI	$GLCD=6218.7RDVI^{2.5689}$	0.7417	774.0064	0.4923	594.8275	(46)
	RVI_2	$GLCD=35.668(RVI_2)^{1.7868}$	0.7955	660.4365	0.6207	487.5695	(47)
	$RVI_{750/700}$	$GLCD=74.588(RVI_{750/700})^{1.7648}$	0.6328	768.3431	0.5215	573.7459	(48)
	$RVI_{800/600}$	$GLCD=48.467(RVI_{800/600})^{1.1957}$	0.6289	758.0084	0.4878	577.4194	(49)
	DVI	$GLCD=10518DVI^{1.7072}$	0.7379	744.1310	0.4471	573.0563	(50)
	TVI	$GLCD=207.25TVI^{11.945}$	0.7378	640.9299	0.6091	511.8146	(51)
	NLI	$GLCD=337.04\exp(2.2699NLI)$	0.7359	671.3678	0.5519	523.6184	(52)
	$RDVI_1$	$GLCD=6357.4(RDVI_1)^{2.289}$	0.7369	692.0701	0.5297	535.1365	(53)
	MSR	$GLCD=171.16MSR^{1.4648}$	0.6933	837.8554	0.5768	620.4622	(54)
	TVI_2	$GLCD=5.4757(TVI_2)^{1.8363}$	0.6769	792.3538	0.3761	614.7573	(55)

The high *R* values of regression models indicate the good relationships between VIs and rice agronomic parameters. For LAI (Table 5), the *R* value is from 0.5844 to 0.6395. Fig.1a shows that there is a tendency for the predictive *LAI* to reach a plateau (around 4.5) after the measured *LAI* greater than 4.5; this tendency indicates that *LAI* would be underestimated at *LAI* greater than 4.5. From Fig.1b, the predictive *LAI* is increased with the increase of the measured *LAI*, the data points are centralized along the line $y=x$; this indicates that the VI of TCARI/OSAVI is a good index for predicting *LAI*. A similar trend exists for RVI_2 (Fig.1c) with TCARI/OSAVI.

For *GLCD* (Table 5), the *R* value is from 0.3761 to 0.7209. From Fig.2a, when the measured *GLCD* is greater than 1 600 mg/m^2, the predictive *GLCD* also reachs a plateau (around 1 500 mg/m^2), this tendency indicates that *GLCD* would be underestimated at *GLCD* greater than 1 600 mg/m^2. From Fig.2b, TCARI/OSAVI has a similar trend with $NDVI_{green}$ for *GLCD*. RVI_2 (Fig.2c) shows that it is also a good index for predicting *GLCD* in that their data points are centralized along $y=x$.

A summary of *ABSE* and *RMSE* for all traditional models is given in Table 5. The lowest *ABSE* and *RMSE* for *LAI* are 1.4003 and 1.1567 on $NDVI_{green}$. The lowest *ABSE* and *RMSE* for *GLCD* are 554.2854 and 427.8513 on TCARI/OSAVI. These results prove that exponent model using $NDVI_{green}$ and exponent model using TCARI/OSAVI are the best models for *LAI* prediction and *GLCD* prediction respectively.

RBF results

RBF with three different algorithms have been applied to evaluate *LAI* and *GLCD* for rice. The best parameters of RBF can be obtained by trial and error. The first sub-dataset (100 samples) are used for building models, and the second sub-dataset (82 samples) for measuring the effectiveness of the models. All calculated results of RBFs are listed in Fig.3, Fig.4 and Table 6. Three different RBFs give three different results for *LAI* and *GLCD*. This phenomenon proves the strong curve fitting ability of RBF, and the predictive results of RBFs should be closer to actual and more accurate.

Fig.3 shows the relationships between predictive *LAI* for the *y* axis and measured *LAI* for the *x* axis by three different RBFs. The results are satisfactory (see Table 6). For three different RBFs using $NDVI_{green}$ (Figs.3a, 3d and 3g), there is a tendency for the predicted *LAI* to be observed reaching a plateau (around 5) after the measured value of *LAI* is greater than 5.5 for ORBF and GDRBF. This tendency indicates that *LAI* would be underestimated when it is greater than 5.5 of GRNN. For different RBFs using TCARI/OSAVI (Figs.3b, 3e and 3h), there is also a tendency for the predicted *LAI* to be underestimated when it is greater than 5.5 for GDRBF and GRNN, but in GRNN the phenomenon underestimating predicted *LAI* does not appear. For different RBFs using RVI_2, their data points are centralized along $y=x$.

Fig.4 shows the relationships between predicted *GLCD* for the *y* axis and measured *GLCD* for the *x* axis by three different RBFs. For three different RBFs using $NDVI_{green}$ (Figs.4a, 4d and 4g), it can be seen that the predicted *GLCD* reachs a plateau (around 1 600) after the measured value of *LAI* reaches greater than 1 800 for all RBFs. This trend indicates that *GLCD* would be underestimated at *GLCD* greater than 1 800. For three RBFs using TCARI/OSAVI (Figs.4b, 4e and 4h), there is also a trend for the predicted *GLCD* to be underestimated at *GLCD* greater than 1 800 for GDRBF and GRNN, but in GRNN the phenomenon of predicted *LAI* to be underestimated does not appear. For different RBFs using RVI_2, their data points are centralized along $y=x$.

The assessment results by *ABSE* and *RMSE* for three different RBFs are given in Table 6. The lowest *ABSE* and *RMSE* for *LAI* are 1.3215 and 1.0728 on ORBF using TCARI/OSAVI. The lowest *ABSE* and *RMSE* for *GLCD* are 527.5001 and 426.5357 on GDRBF using TCARI/OSAVI. These results prove that TCARI/OSAVI is the best index for *LAI* prediction and *GLCD* prediction in RBF.

Comparison of traditional models and RBF

The two different methods including traditional models and RBF gave different *RMSE* and *ABSE* in the same circumstances (Table 7). For traditional models, the exponent model using $NDVI_{green}$ provided the best result for *LAI* prediction, and the exponent model using TCARI/OSAVI provided the best result for *GLCD* prediction. But for different RBFs, the GDRBF using $NDVI_{green}$ provided higher *RMSE* (1.3708) and *ABSE* (1.1344) than the other two RBFs using $NDVI_{green}$ for

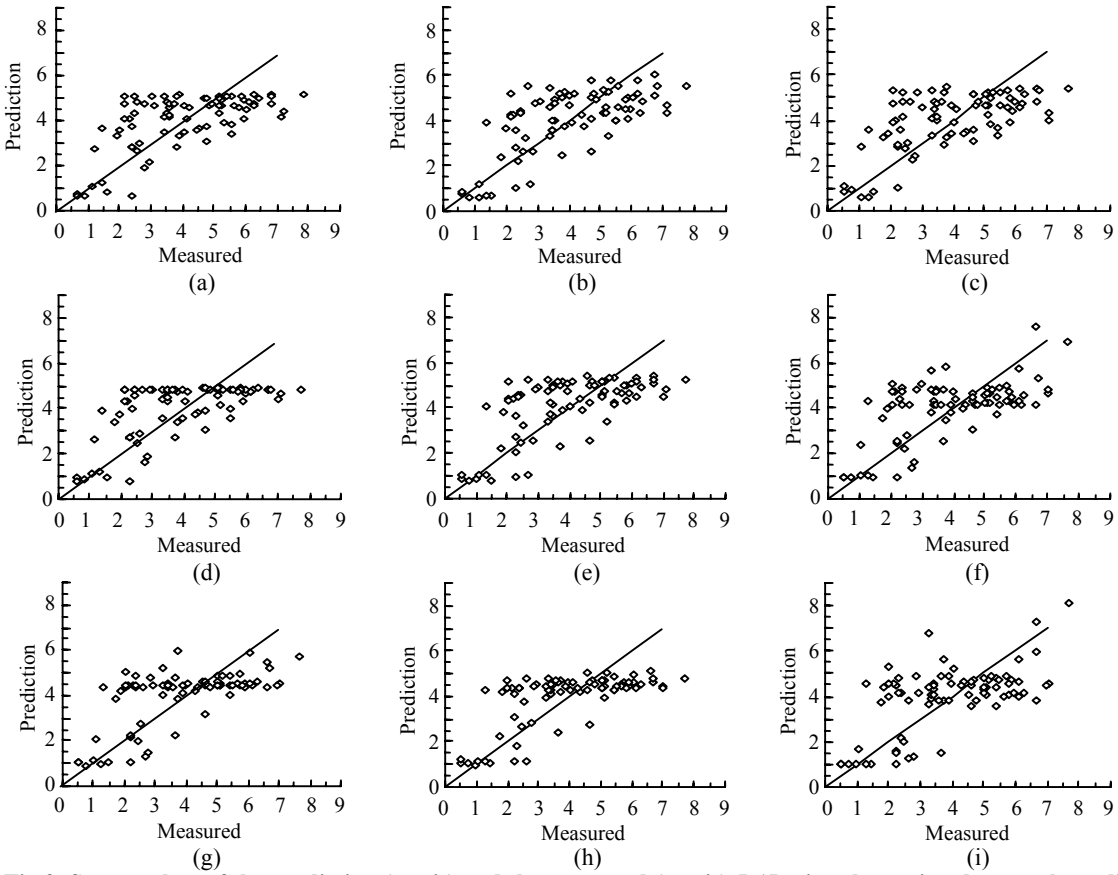

Fig.3 Scatter plots of the prediction (*y* axis) and the measured (*x* axis) *LAI* using the testing data on three different RBFs. From left to right, the columns are $NDVI_{green}$, TCARI/OSAVI and RVI_2. The top row is for ORBF, the middle row for GDRBF and the bottom row for GRNN. The line is *y=x*

Table 6 The assessment results of three different RBFs for *LAI* and *GLCD* of rice

	Vegetation Index	ORBF			GDRBF			GRNN		
		RMSE	*R*	*ABSE*	*RMSE*	*R*	*ABSE*	*RMSE*	*R*	*ABSE*
LAI	$NDVI_{green}$	1.3805	0.6188	1.1236	**1.3708**	**0.6169**	**1.1344**	1.3785	0.6149	1.1317
	TCARI/OSAVI	**1.3215**	**0.6648**	**1.0728**	1.3311	0.6550	1.0703	1.3386	0.6360	1.1074
	RVI_2	**1.3722**	**0.6199**	**1.1303**	1.3909	0.6147	1.1436	1.4249	0.6106	1.1518
GLCD	*RVI*	**609.0749**	**0.6079**	**507.7887**	638.1222	0.5546	516.9093	624.4176	0.5905	514.8191
	NDVI	602.2513	0.6228	500.6547	**602.2531**	**0.6263**	**493.6171**	609.3889	0.6169	499.4114
	$NDVI_{green}$	542.3022	0.7041	437.7037	544.7337	0.7032	436.4759	**532.1145**	**0.7192**	**427.7069**
	SAVI	**602.2768**	**0.6228**	**500.6666**	632.3894	0.5627	500.3948	609.4043	0.6170	499.3955
	OSAVI	624.6131	0.5892	517.1805	592.7082	0.6377	474.9739	**591.6998**	**0.6440**	**475.9692**
	MSAVI	611.4533	0.6047	484.4775	**604.0929**	**0.6157**	**468.2026**	611.1092	0.6073	480.1518
	MCACI	**625.7129**	**0.6002**	**509.7786**	664.3278	0.5079	537.8178	637.6536	0.5636	507.6971
	TCARI/OSAVI	528.6849	0.7211	424.6719	**527.5001**	**0.7244**	**426.5357**	556.4677	0.6814	433.3864
	RDVI	595.2044	0.6368	474.8368	**595.1046**	**0.6369**	**474.7572**	603.6108	0.6236	484.9673
	RVI_2	552.0848	0.6967	462.0266	559.2210	0.6798	442.2226	**532.2058**	**0.7203**	**422.4157**
	$RVI_{750/700}$	**605.9865**	**0.6236**	**491.8612**	640.5341	0.5620	498.7388	614.2547	0.5981	483.3580
	$RVI_{800/600}$	**624.4980**	**0.5900**	**515.6861**	666.9507	0.5192	523.5025	636.3517	0.5617	512.3777
	DVI	615.2747	0.5997	482.6309	**613.1627**	**0.6040**	**480.3562**	630.2224	0.5758	503.3632
	TVI	**601.6319**	**0.6235**	**499.8519**	626.8007	0.5674	504.7917	619.1016	0.5897	507.9827
	NLI	606.2859	0.6179	499.4349	617.4466	0.5954	485.2148	**601.7019**	**0.6231**	**484.1142**
	$RDVI_1$	**586.3177**	**0.6455**	**466.5682**	600.6685	0.6171	464.7354	595.1132	0.6334	475.4493
	MSR	**608.7430**	**0.6187**	**503.2635**	733.4580	0.4506	564.8670	642.6542	0.5533	519.6060
	TVI_2	660.2811	0.5336	538.7333	659.5891	0.5141	519.9785	**632.8077**	**0.5722**	**504.4340**

Note: the highlighted data denote the best result among the three different RBFs using the same VI

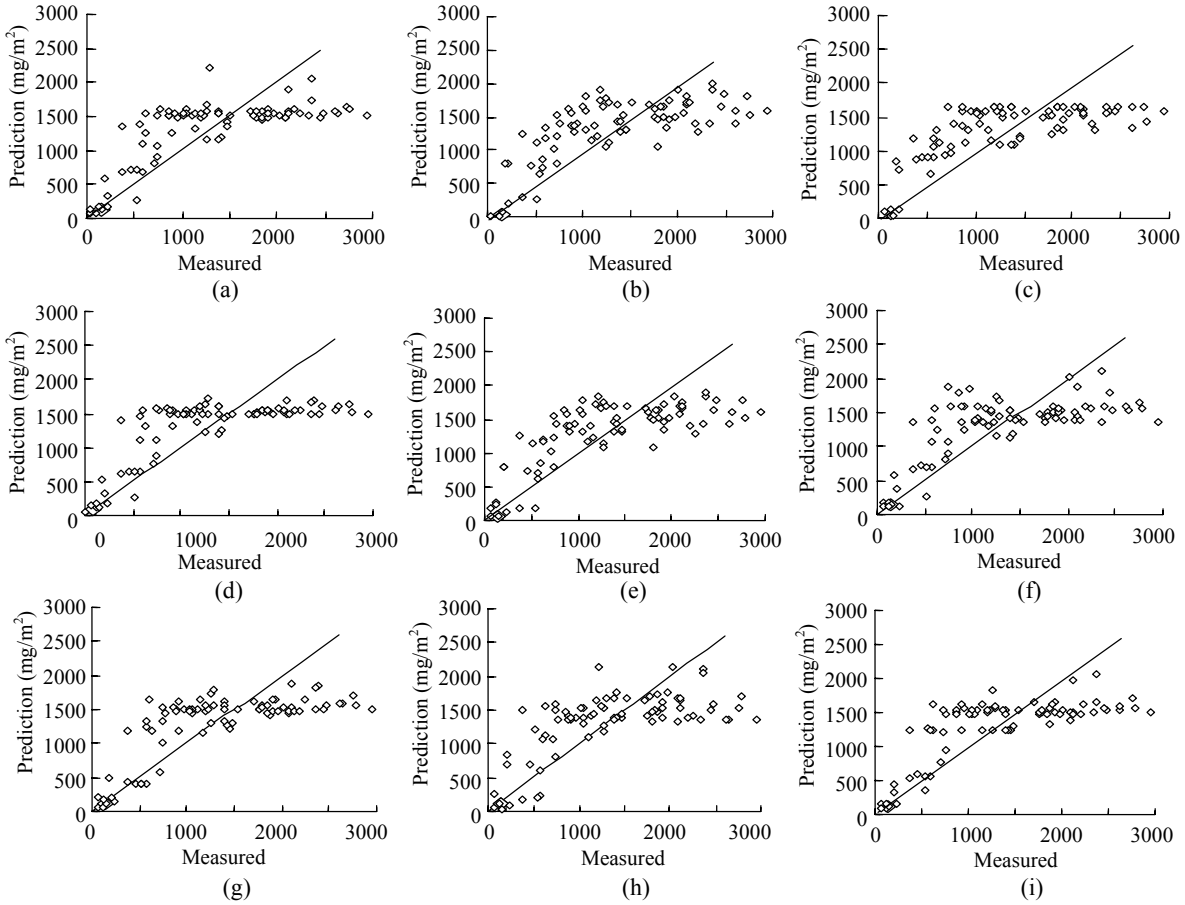

Fig.4 Scatter plots of the prediction (*y* axis) and the measured (*x* axis) *GLCD* using the testing data on three different RBFs only for three VIs. From left to right, the columns are $NDVI_{green}$, TCARI/OSAVI and RVI_2. The top row is for ORBF, the middle row for GDRBF and the bottom row for GRNN. The line is *y=x*

LAI, the ORBF using TCARI/OSAVI provided the lowest *RMSE* (1.3215) and the lowest *ABSE* (1.0728) for *LAI* than the other two RBFs, and the GDRBF using TCARI/OSAVI provided the lowest *RMSE* (527.5001) and the lowest *ABSE* (426.5357) for *GLCD* prediction than the others.

The performances of the best RBF were compared with the results obtained in the best traditional models. Significant improvement was observed for *LAI* where *RMSE* and *ABSE* decreased from 1.4003 and 1.1567 in traditional models to 1.3708 and 1.1344 in GDRBF using $NDVI_{green}$ respectively, and *RMSE* and *ABSE* decreased from 1.4334 and 1.1905 in traditional models to 1.3215 and 1.0728 in ORBF using TCARI/OSAVI respectively. Especially, the most significant improvement was also observed for *GLCD* where *RMSE* and *ABSE* decreased from 554.2854 and 427.8513 in traditional models to 528.6849 and 424.6719 in ORBF using TCARI/OSAVI, *RMSE* and *ABSE* decreased from 554.2854 and 427.8513 in traditional models to 527.5001 and 426.5357 in GDRBF using TCARI/OSAVI. Compared with the values of *RMSE* and *ABSE* of all models using different VIs, all RBFs can further improve the relationships between all VIs and agronomic parameters excluding the GRNN using TCARI/OSAVI. Therefore, the relationships between VIs and agronomic parameters have been improved by RBF methods.

DISCUSSION AND CONCLUSION

In the present work, 25 different VIs were used to compare prediction power to rice *LAI* and rice *GLCD* (Table 2). The $NDVI_{green}$ and TCARI/OSAVI are the best indices to estimate the rice *LAI* by exponent model and ORBF respectively. The TCARI/OSAVI is the best index to estimate the rice *GLCD* by exponent model and RBF.

Table 7 The increase in traditional models over three RBFs on *RMSE* and *ABSE*

	Vegetation Index	ORBF		GDRBF		GRNN	
		Δ*RMSE*	Δ*ABSE*	Δ*RMSE*	Δ*ABSE*	Δ*RMSE*	Δ*ABSE*
LAI	$NDVI_{green}$	0.0198	0.0331	0.0295	0.0223	0.0218	0.025
	TCARI/OSAVI	0.1119	0.1177	0.1023	0.1202	0.0948	0.0831
	RVI_2	0.1121	0.0470	0.0934	0.0337	0.0594	0.0255
GLCD	*RVI*	145.8884	56.9919	116.8411	47.8713	130.5457	49.9615
	NDVI	36.5677	11.1063	36.5659	18.1439	29.4301	12.3496
	$NDVI_{green}$	24.2840	1.5754	21.8525	2.8032	34.4717	11.5722
	SAVI	36.6425	11.1212	6.5299	11.3930	29.5150	12.3923
	OSAVI	55.0531	10.3415	86.9580	52.5481	87.9664	51.5528
	MSAVI	118.8995	80.4476	126.2599	96.7225	119.2436	84.7733
	MCACI	97.9556	59.4599	59.3407	31.4207	86.0149	61.5414
	TCARI/OSAVI	25.6005	3.1794	26.7853	1.3156	−2.1823	−5.5351
	RDVI	178.8020	119.9907	178.9018	120.0703	170.3956	109.8602
	RVI_2	108.3517	25.5429	101.2155	45.3469	128.2307	65.1538
	$RVI_{750/700}$	162.3566	81.8847	127.8090	75.0071	154.0884	90.3879
	$RVI_{800/600}$	133.5104	61.7333	91.0577	53.9169	121.6567	65.0417
	DVI	128.8563	90.4254	130.9683	92.7001	113.9086	69.6931
	TVI	39.2980	11.9627	14.1292	7.0229	21.8283	3.8319
	NLI	65.0819	24.1835	53.9212	38.4036	69.6659	39.5042
	$RDVI_1$	105.7524	68.5683	91.4016	70.4011	96.9569	59.6872
	MSR	229.1124	117.1987	104.3974	55.5952	195.2012	100.8562
	TVI_2	132.0727	76.0240	132.7647	94.7788	159.5461	110.3233

Note: Δ denotes the increase in traditional models over three different RBFs on *RMSE* and *ABSE*

RBF, from now on, has only been used in a few domains within remote sensing in agriculture. The present work represents an initial step in evaluating RBF compared to traditional models.

RBF performs better (the ORBF using TCARI/OSAVI improve 0.1119 and 0.1177 for *LAI* by *RMSE* and *ABSE* respectively, the GDRBF using TCARI/OSAVI improve 26.7853 and 1.3156 for *GLCD* by *RMSE* and *ABSE* respectively) compared with the traditional regression based on the best VIs in this study showing that RBF is indeed a potentially useful method. It is very critical to select the correct RBF algorithm in order to avoid 'over-fitting'. Three different algorithms were selected for *LAI* and *GLCD*. These two variables, at the same time, were those in which the highest improvement was observed. Consequently, RBF provides a useful explorative tool for improvement of the relationships between VIs and crop variables. Much work still remains to be done to scale these greenness estimation relationships among various canopies, so larger scale remote sensing may be put into application.

ACKNOWLEDGEMENT

We gratefully acknowledge the data providers including Qiuxiang Yi, Yuan Wang, Fuming Wang of the Institute of Agricultural Remote Sensing & Information Application, Huajiachi Campus, Zhejiang University, Hangzhou, China.

References

Ahlrichs, J.S., Bauer, M.E., 1983. Relation of agronomic and multispectral reflectance characteristics of spring wheat canopies. *Agronomy Journal*, **75**:987-993.

Aparicio, N., Villegas, D., Casadesus, J., Araus, J.L., Royo, C., 2000. Spectral vegetation indices as non-destructive tools for determining durum wheat yield. *Agronomy Journal*, **92**:83-91.

Asseng, S., Keulen, H., Stol, W., 2000. Performance and application of the APSIMN wheat model in the Netherlands. *European Journal of Agronomy*, **12**:37-54. [doi:10.1016/S1161-0301(99)00044-1]

Best, R.G., Harlan, J.C., 1985. Spectral estimation of green leaf area index of oats. *Remote Sensing of Environment*, **17**:27-36. [doi:10.1016/0034-4257(85)90110-5]

Boegh, E., Soegaard, H., Broge, N., Hasager, C.B., Jensen, N.O., Schelde, K., Thomsen, A., 2002. Airborne multis-

pectral data for quantifying leaf area index, nitrogen concentration, and photosynthetic efficiency in agriculture. *Remote Sensing of Environment*, **81**:179-193. [doi:10.1016/S0034-4257(01)00342-X]

Bors, A.G., Gabbouj, G., 1994. Minimal topology for a radial basis function neural network for pattern classification. *Digital Signal Processing*, **4**(3):173-188. [doi:10.1006/dspr.1994.1016]

Bors, A.G., Pitas, I., 1996. Median radial basis functions neural network. *IEEE Trans. on Neural Networks*, **7**(6):1351-1364. [doi:10.1109/72.548164]

Bors, A.G., Pitas, I., 1998. Optical flow estimation and moving object segmentation based on median radial basis function network. *IEEE Trans. on Image Processing*, **7**(5):693-702. [doi:10.1109/83.668026]

Bors, A.G., Pitas, I., 1999. Object classification in 3-D images using alpha-trimmed mean radial basis function network. *IEEE Trans. on Image Processing*, **8**(12):1744-1756. [doi:10.1109/83.806620]

Broge, N.H., Leblanc, E., 2001. Comparing prediction power and stability of broadband and hyperspectral vegetation indices for estimation of green leaf area index and canopy chlorophyll density. *Remote Sensing of Environment*, **76**:156-172. [doi:10.1016/S0034-4257(00)00197-8]

Broge, N.H., Mortensen, J.V., 2002. Deriving green crop area index and canopy chlorophyll density of winter wheat from spectral reflectance data. *Remote Sensing of Environment*, **81**:45-57. [doi:10.1016/S0034-4257(01)00332-7]

Broomhead, D.S., Lowe, D., 1988. Multivariable functional interpolation and adaptive networks. *Complex Systems*, **2**:321-355.

Casdagli, M., 1989. Nonlinear prediction of chaotic time series. *Phys. D*, **35**:335-356. [doi:10.1016/0167-2789(89)90074-2]

Cha, I., Kassam, S.A., 1996. RBFN restoration of nonlinearly degraded images. *IEEE Trans. on Image Processing*, **5**(6):964-975. [doi:10.1109/83.503912]

Chatzis, V., Bors, A.G., Pitas, I., 1999. Multimodal decision-level fusion for person authentification. *IEEE Trans. on Systems, Man, and Cybernetics, Part A: Systems and Humans*, **29**(6):674-680. [doi:10.1109/3468.798073]

Chen, S., Cowan, C.F.N., Grant, P.M., 1991. Orthogonal least squares learning algorithm for radial basis function networks. *IEEE Trans. on Neural Networks*, **2**(2):302-309. [doi:10.1109/72.80341]

Cheng, Q., Huang, J., Wang, X., Wang, R., 2003. In situ hyperspectral data analysis for pigment content estimation of rice leaves. *J. Zhejiang Univ. Sci.*, **4**(6):727-733.

Cheng, Q., 2006. Multisensor comparisons for validation of MODIS vegetation indices. *Pedosphere*, **16**(3):362-370. [doi:10.1016/S1002-0160(06)60064-7]

Christensen, S., Goudriaan, J., 1993. Deriving light interception and biomass from spectral reflectance ratio. *Remote Sensing of Environment*, **43**:87-95. [doi:10.1016/0034-4257(93)90066-7]

Curran, P.J., Dungan, J.L., Peterson, D.L., 2001. Estimating the foliar biochemical concentration of leaves with reflectance spectrometry-testing the Kolaly and Clark methodologies. *Remote Sensing of Environment*, **76**:349-359. [doi:10.1016/S0034-4257(01)00182-1]

Daughtry, C.S.T., Walthall, C.L., Kim, M.S., Brown de Colstoun, E., McMurtrey III, J.E., 2000. Estimating corn leaf chlorophyll concentration from leaf and canopy reflectance. *Remote Sensing of Environment*, **74**:229-239. [doi:10.1016/S0034-4257(00)00113-9]

Gitelson, A.A., Kaufman, Y.J., Merzlyak, M.N., 1996. Use of a green channel in remote sensing of global vegetation from EOS-MODIS. *Remote Sensing of Environment*, **58**:289-298. [doi:10.1016/S0034-4257(96)00072-7]

Gitelson, A.A., Kaufman, Y.J., Stark, R., Rundquist, D., 2002. Novel algorithm for remote estimation of vegetation fraction. *Remote Sensing of Environment*, **80**:76-87. [doi:10.1016/S0034-4257(01)00289-9]

Goel, N.S., Qi, W., 1994. Influences of canopy architecture on relationships between various vegetation indices and LAI and FPAR: a computer simulastion. *Remote Sensing of Environment*, **10**:309-347.

Gong, P., Pu, R., Binging, G.S., Larrieu, M.R., 2003. Estimation of forest leaf area index using vegetation indices derived from hyperion hyperspectral data. *IEEE Trans. on Geoscience and Remote Sensing*, **41**(6):1355-1362. [doi:10.1109/TGRS.2003.812910]

Haboudane, D., Miller, J.R., Tremblay, N., Zarco-Tejada, P.J., Dextraze, L., 2002. Integrated narrow-band vegetation indices for prediction of crop chlorophyll content for application to precision agriculture. *Remote Sensing of Environment*, **81**:416-426. [doi:10.1016/S0034-4257(02)00018-4]

Haykin, S., 1994. Neural Networks: A Comprehensive Foundation. Upper Saddle River, Prentice Hall, NJ.

Huete, A.R., 1988. A soil-adjusted vegetation index (SAVI). *Remote Sensing of Environment*, **25**:295-309. [doi:10.1016/0034-4257(88)90106-X]

Jamieson, P.D., Porter, J.R., Goudrian, J., Ritchie, J.T., Keulen, H., Stol, W., 1998. A comparison of the models AFRCWHEAT2, CERES-wheat, Sirius, SUCROS2 and SWHEAT with measurements from wheat grown under drought. *Field Crops Research*, **55**:23-44. [doi:10.1016/S0378-4290(97)00060-9]

Jordan, C.F., 1969. Derivation of leaf area index from quality of light on the forest floor. *Ecology*, **50**:663-666. [doi:10.2307/1936256]

Kim, M.S., Daughtry, C.S.T., Chappelle, E.W., McMurtrey III, J.E., Walthall, C.L., 1994. The Use of High Spectral Resolution Bands for Estimating Absorbed Photosynthetically Active Radiation (Apar). Proc. 6th Symposium on Physical Measurements and Signatures in Remote Sensing. Val D'Isere, France, p.299-306.

Kohonen, T.K., 1989. Self-organization and Associative Memory. Springer-Verlag, Berlin.

Lukina, E.V., Stone, M.L., Raun, W.R., 1999. Estimating vegetation coverage in wheat using digital images. *J. Plant Nutr.*, **22**:341-350.

Matej, S., Lewitt, R.M., 1996. Practical considerations for 3-D image reconstruction using spherically symmetric volume

elements. *IEEE Trans. on Medical Imaging*, **15**(1):68-78. [doi:10.1109/42.481442]

Moody, J., 1989. Fast learning in networks of locally-tuned processing units. *Neural Computation*, **1**:281-294.

Musavi, M.T., Ahmed, W., Chan, K.H., Faris, K.B., Hummels, D.M., 1992. On the training of radial basis function classifiers. *Neural Networks*, **5**:595-603. [doi:10.1016/S0893-6080(05)80038-3]

Mutanga, O., Skidmore, A.K., 2004. Integrating imaging spectroscopy and neural networks to map grass quality in the Kruger National Park, South Africa. *Remote Sensing of Environment*, **90**:104-115. [doi:10.1016/j.rse.2003.12.004]

Niranjan, M., Fallside, F., 1990. Neural networks and radial basis functions in classifying static speech patterns. *Computer Speech and Language*, **4**:275-289. [doi:10.1016/0885-2308(90)90009-U]

O'Neal, M.R., Engel, B.A., Ess, D.R., Frankenberger, J.R., 2002. Neural network prediction of maize yield using alternative data coding algorithms. *Biosystems Engineering*, **83**(1):31-45. [doi:10.1006/bioe.2002.0098]

Park, J., Sandberg, J.W., 1991. Universal approximation using radial basis functions network. *Neural Computation*, **3**:246-257.

Pearson, R.L., Miller, L.D., 1972. Remote Mapping of Standing Crop Biomass for Estimation of the Productivity of the Short-grass Prairie, Pawnee National Grasslands, Colorado. Proc. 8th International Symposium on Remote Sensing of Environment, p.1357-1381.

Peñuelas, J., Baret, F., Filella, I., 1995. Semi-empirical indices to assess carotenoids/chlorophyll a ratio from leaf spectral reflectance. *Photosynthetica*, **31**(2):221-230.

Poggio, T., Girosi, F., 1990. Networks for approximation and learning. *Proc. IEEE*, **78**(9):1481-1497. [doi:10.1109/5.58326]

Qi, J., Chehbouni, A., Huete, A.R., Kerr, Y.H., Sorooshian, S., 1994. A modified soil adjusted vegetation index. *Remote Sensing of Environment*, **48**:119-126. [doi:10.1016/0034-4257(94)90134-1]

Rondeaux, G., Steven, M., Baret, F., 1996. Optimization of soil-adjusted vegetation indices. *Remote Sensing of Environment*, **55**:95-107. [doi:10.1016/0034-4257(95)00186-7]

Roujean, J.L., Breon, F.M., 1995. Estimating PAR absorbed by vegetation from bidirectional reflectance measurements. *Remote Sensing of Environment*, **51**(3):375-384. [doi:10.1016/0034-4257(94)00114-3]

Rouse, J.W., Haas, R.H., Schell, J.A., Deering, D.W., Harlan, J.C., 1974. Monitoring the Vernal Advancements and Retrogradation of Natural Vegetation. NASA/GSFC, Final Report. Greenbelt, MD, USA, p.1-137.

Sanner, R.M., Slotine, J.E., 1992. Gaussian networks for direct adaptive control. *IEEE Trans. on Neural Networks*, **3**(6):837-863. [doi:10.1109/72.165588]

Serrano, L., Filella, I., Peñuelas, J., 2000. Remote sensing of biomass and yield of winter wheat under different nitrogen supplies. *Crop Sci.*, **40**:723-731.

Sims, D.A., Gamon, J.A., 2002. Relationships between leaf pigment content and spectral reflectance across a wide range of species, leaf structures and developmental stages. *Remote Sensing of Environment*, **81**(2-3):337-354. [doi:10.1016/S0034-4257(02)00010-X]

Tang, Y., Wang, R., Huang, J., 2004. Relations between red edge characteristics and agronomic parameters of crop. *Pedosphere*, **4**(4):467-474.

Thenkabail, P.S., Smith, R.B., de Pauw, E., 2000. Hyperspectral vegetation indices and their relationships with agricultural crop characteristics. *Remote Sensing of Environment*, **71**:158-182. [doi:10.1016/S0034-4257(99)00067-X]

Tou, J.T., Gonzalez, R.C., 1974. Pattern Recognition. Reading, Addison-Wesley, MA.

Wei, G.Q., Hirzinger, G., 1997. Parametric shape-from-shading by radial basis functions. *IEEE Trans. on Patt. Anal. & Machine Intell.*, **19**(4):353-365. [doi:10.1109/34.588016]

Yang, X., Huang, J., Wang, F., Wang, X., Yi, Q., Wang, Y., 2006. A modified chlorophyll absorption continuum index for chlorophyll estimation. *J. Zhejiang Univ. Sci. A*, **7**(12):2002-2006. [doi:10.1631/jzus.2006.A2002]

Zhang, J., Wang, K., Bailey, J.S., Wang, R., 2006. Predicting nitrogen status of rice using multispectral data at canopy scale. *Pedosphere*, **16**(1):108-117. [doi:10.1016/S1002-0160(06)60032-5]